

Condensation–Sorting Events in the Rough Endoplasmic Reticulum of Exocrine Pancreatic Cells

John Tooze,* Horst F. Kern,‡ Stephen D. Fuller,* and Kathryn E. Howell*

*European Molecular Biology Laboratory, 6900 Heidelberg, Federal Republic of Germany; and ‡University of Marburg, Marburg, Federal Republic of Germany

Abstract. In guinea pig exocrine pancreatic cells intracisternal granules (ICGs) occur at a low frequency within the lumen of the RER. By starving and refeeding guinea pigs or injecting them in CoCl_2 solution, the number of these granules is greatly increased. We show here that ICGs contain the complete set of secreted pancreatic digestive enzymes and proenzymes. Two other soluble proteins in the lumen of the RER, GRP 78/BiP and protein disulphide isomerase (PDI), are specifically excluded from ICGs. The formation of ICGs, which occurs without acidification of the RER cisternae, is therefore a sorting event involving the cocondensation of a complete set of secretory enzymes and proenzymes, which for brevity we refer to collectively as the zymogens. With the exception of $\sim 50\%$ of the RNase, the zymogens in ICGs are covalently cross-linked by intermolecular disulphide bonds. The synthesis of all three resident ER cisternal proteins—

PDI, GRP 78/BiP, and GRP 94—with the carboxy-terminal sequence KDEL, is induced in response to the accumulation of massive amounts of misfolded secretory protein in the ICGs in the lumen of the RER. After injection of rats with large doses of parachlorophenylalanine-methylester, crystals form in the lumen of the RER. We show that these crystals appear to be a lattice of amylase with the other zymogens incorporated between the layers. Both GRP 78/BiP and PDI are excluded from these crystals. The formation of these amylase crystals within the RER and the inclusion of other zymogens is, therefore, also a sorting event. These data establish that in exocrine pancreatic cells zymogens can cocondense in the RER into either amorphous aggregates or crystals that exclude other soluble RER proteins. This demonstrates that cocondensation is a mechanism capable of sorting zymogens within the secretory pathway.

THE condensation of proteins secreted via the regulated pathway into osmotically inert cores of secretory granules could both concentrate these proteins and sort them from resident and constitutively secreted proteins. If regulated secretory proteins are inherently prone to coaggregate and come out of solution when they reach locally high concentrations, whereas other proteins lack this property, it follows that whenever and wherever condensation occurs it will sort the regulated proteins from the rest. Evidence, mostly morphological, relevant to this long-standing idea—the condensation–sorting hypothesis—has recently been reviewed (8).

In both exocrine and endocrine cells, condensation of regulated secretory proteins into secretory granule cores usually occurs in *trans* Golgi compartments (16). This implies that the critical concentration for condensation to occur is normally reached first in the *trans* Golgi compartment. In endocrine cells, regulated secretory proteins are concentrated ~ 200 -fold between the RER and the *trans* Golgi compartment (45), while in exocrine cells the concentration

factor is ~ 10 -fold (4). It has been proposed that acidic glucosaminoglycans may also play a role in the concentration of pancreatic secretory proteins (43, 44). If, however, the critical concentration for condensation were to be reached earlier in the exocytic pathway, condensation should also occur earlier. Premature condensation is indeed observed under certain conditions. For example, hyperstimulation of hypothalamic neurons leads to condensation of vasopressin and oxytocin in the medial and *cis* Golgi cisternae (7). In thyrotrophs in the pituitary of thyroidectomized mice, condensation of protein into intracisternal granules (ICGs)¹ occurs even in the RER (14, 15). ICGs can also develop in the RER of cells of the pars intermedia of *Xenopus laevis* pituitary after stimulation of synthesis of melanocyte-stimulating hormone (22). Farquhar (14, 15) proposed that in these endocrine cells, after hyperstimulation, the rate of export of secretory proteins from the RER fails to keep pace with the rate of synthesis, and as a result secretory proteins condense into ICGs.

K. E. Howell's present address is Department of Cellular and Structural Biology, University of Colorado Medical School, Denver, CO 80262.

1. *Abbreviations used in this paper:* DAMP, 3-C2,4-dinitroanilino-3'-amino-N-methylpropylamine; ICG, intracisternal granule; PDI, protein disulphide isomerase.

Under some conditions ICGs also form in exocrine pancreatic cells. In the guinea pig exocrine pancreas, for example, as Palade (37) first observed, spherical granules resembling the cores of zymogen granules occur in the RER of some cells. Immunocytochemistry (20) showed that these granules contain chymotrypsinogen. The frequency of ICGs is greatly increased by a simple and physiological manipulation: if guinea pigs are starved for 1–2 d and then refed, many ICGs form within 1–2 h of refeeding (20, 37). This induction of ICGs is readily explainable. Synthesis of pancreatic digestive enzymes and proenzymes, for brevity referred to here collectively as zymogens, is down regulated during starvation; refeeding leads to an increase in synthesis, and in many cells the concentration at which zymogens condense is apparently reached in the RER. ICGs can also be experimentally induced in guinea pigs by injecting CoCl_2 solutions (25). The Co^{++} must somehow inhibit the export of zymogens from the RER. The Golgi complex decreases in size and condensing vacuoles no longer form. Instead, virtually all of the exocrine cells have ICGs throughout their RER.

ICGs are rare in rat exocrine pancreatic cells; however, under certain conditions crystallization of zymogens occurs in the RER. For example, in primary cultures of fetal rat exocrine pancreatic cells, treatment with dexamethasone leads to a 10-fold increase in the content of amylase and a smaller increase in other zymogens; it also results in crystals forming within the RER cisternae (41). Incubation of rat pancreatic lobules in media containing colchicine or vinblastine inhibits the stimutable release of pulse-labeled zymogens, and, concomitantly, crystals form in the RER (49). Similar zymogen crystals also form when adult rats are injected with large doses of aromatic amino acids (17). Rat and guinea pig exocrine pancreas provide, therefore, two convenient experimental systems in which to study two different types of condensation of zymogens in the RER.

Clearly, the condensation of regulated secretory proteins is not restricted to the *trans* Golgi network. The condensation–sorting hypothesis predicts that once regulated proteins reach a critical concentration in any compartment they should come out of solution. But are ICGs or crystals in the RER of exocrine pancreatic cells sorted, as the hypothesis also predicts? Do they exclude resident or constitutively secreted proteins while containing all the zymogens? Here we show that two abundant soluble proteins found only in the lumen of the ER (34, 35, 39)—i.e., GRP 78/BiP and protein disulphide isomerase (PDI)—are indeed specifically excluded from ICGs in guinea pig pancreatic cells and from zymogen crystals in rat pancreatic cells.

Materials and Methods

Induction of ICGs

Young guinea pigs weighing 200–250 g (Charles River Vega GmbH, Sulzfeld, FRG) were injected subcutaneously with CoCl_2 in 0.9% sterile saline at a dose of 15 mg/kg body weight at the same time on three consecutive days. The animals were killed by a blow on the head 24 h after the last injection of CoCl_2 . The pancreas was removed and lobules were prepared (47). Alternatively guinea pigs were fasted for 24–48 h, allowed to feed for 1 h, and then killed.

Induction of Zymogen Crystals

Rats weighing ~200 g (Charles River Vega GmbH) were injected in-

traperitoneally with a single dose (50 mg/100 g body weight) of DL-4-chlorophenylalanine-methylester-HCl (Serva Fine Biochemicals Inc., Heidelberg, FRG) and decapitated 24 h later. Lobules were then prepared from the pancreas (47).

Incubation Experiments

Guinea pig pancreatic lobules were incubated in 15 ml labeling media consisting of MEM minus methionine and cysteine (Gibco Laboratories, Grand Island, NY), 0.1% BSA, 0.01% soybean trypsin inhibitor, 24 mM Hepes, pH 7.4, containing 300 μCi each of [^{35}S]methionine and [^{35}S]cysteine (Amersham International, Amersham, UK). The lobules were oxygenated and metabolically labeled at 37°C. At 15-, 30-, 45-, and 60-min time points, 10 lobules were removed and the flasks were reoxygenated. The removed lobules were washed in quenching medium containing a 10-fold excess of unlabeled methionine and cysteine, and homogenized in 2 ml of 0.2 M NaHCO_3 , pH 8, in a homogenizer (AA glass/Teflon; A. H. Thomas, Philadelphia, PA). The ensuing homogenate was frozen in aliquots in liquid nitrogen. To study the effect of Co^{++} ions on protein synthesis, intracellular transport, and respiration, lobules were incubated in media containing [^3H]leucine and [^{14}C]palmitate (Amersham International) according to Jamieson and Palade (23).

Analysis of Radiolabeled Protein

Protein assays were carried out on each sample (6) using bovine γ globulin as a standard: 100- μg samples were prepared and run on 5–15% acrylamide gradient gels (31). Entensify (New England Nuclear, Boston, MA) and X-Omat film AR 5 (Eastman Kodak Co., Rochester, NY) were used for the enhancement and detection of the label in the gels. To quantitate the amount of label in individual bands, the autoradiograph was used as the template and the labeled bands were excised from the gel and solubilized in 1 ml 30% H_2O_2 at 70°C overnight. Scintillation cocktail was then added and the samples were counted.

For immunoblots, duplicate gels were run, transferred to nitrocellulose (9) (90 mA, overnight), and quenched with 10% low-fat milk in PBS. The dilution of the antiserum (anti-guinea pig zymogen granule content, anti-BiP, and anti-PDI) was 1:100 in 10% low-fat milk in PBS. Detection was with goat anti-rabbit IgG antibody conjugated to horseradish peroxidase (BioSystems, Compiègne, France) and the peroxidase histochemical reaction.

Isolation of Zymogen Granules and ICGs

Zymogen granules from the pancreas of normal guinea pigs were isolated (50). To isolate the ICGs, pancreas was removed from cobalt-treated guinea pigs, minced, and 1 g wet weight tissue was homogenized in 10 ml of 0.3 M sucrose at 4°C with 4 strokes of a homogenizer (B glass/Teflon; A. H. Thomas). The homogenate was centrifuged at 600 g for 10 min, and the resulting supernatant was subjected to a second centrifuge at 1,000 g for 10 min. The supernatant was removed and pelleted at 100,000 g for 1 h in a rotor (70Ti; Beckman Instruments, Inc., Fullerton, CA). The resulting pellet was resuspended in 0.3 M sucrose, loaded on a continuous gradient of 1.5–2.5 M sucrose in tubes for a rotor (SW40; Beckman Instruments, Inc.), and centrifuged at 100,000 g overnight. ICGs were recovered from two distinct bands at densities of 1.25 and 1.26 g/ml. The fractions were assessed by electron microscopy and SDS-PAGE.

Analysis of Zymogen Granule and ICG Content

Zymogen granule fractions were lysed in 0.2 M NaH_2CO_3 , pH 8, for 1 h at 4°C. The lysate was centrifuged to pellet the membranes, and the supernatant containing all the zymogens was separated into equal portions and prepared under reducing and nonreducing conditions in SDS-gel electrophoresis sample buffer (31) containing 50 mM Tris-HCl buffer, pH 6.8, 5 mM EDTA, 300 mM sucrose, and 2% SDS with 30 mM DTT in the reduced samples. The samples were heated to 95°C for 1 min, cooled, and 30 mM iodoacetic acid was added. Since the electron microscopic analysis of the ICG fractions showed that very few RER membranes were present, the NaH_2CO_3 lysis step was omitted and the fraction was solubilized directly in either reducing or nonreducing sample buffer and analyzed by SDS-PAGE. In other experiments ICGs were washed in PBS containing 10 mM Mg ATP. The solubilized proteins were analyzed by SDS-PAGE, and the insoluble pellet of granules was dissolved in reducing sample buffer and analyzed in parallel.

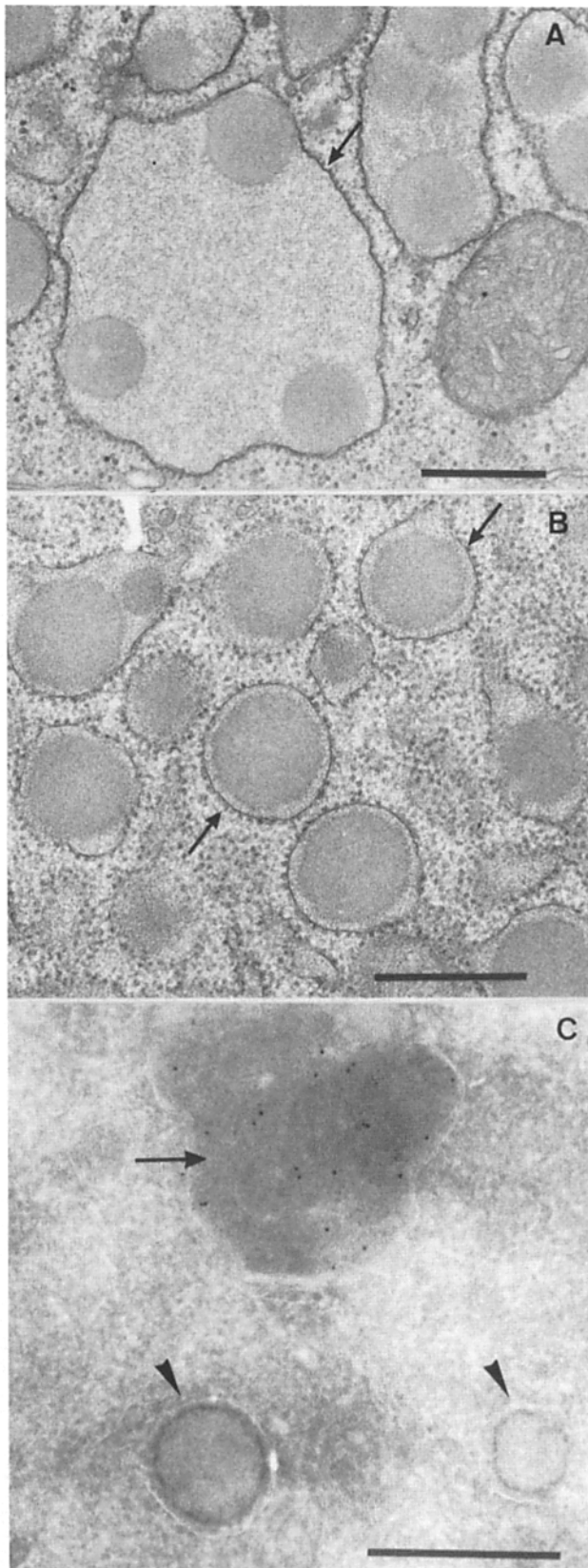


Figure 1. ICGs in the RER. After their induction by injections of CoCl_2 (A) or starvation-refeeding (B), spherical ICGs accumulate throughout the lumen of the RER of guinea pig exocrine pancreatic cells. Note the distended cisterna containing three ICGs in A. Serial sections show that the RER cisternae are not vesiculated: profiles such as those shown in B are sections transverse to the long axis

Production of Antibodies

Antiserum against PDI, purified from rat liver by the procedure of Lambert and Freedman (28), was raised in a rabbit using the protocol of Louvard et al. (29). Antisera against synthetic peptides with the carboxy-terminal sequences of rat PDI, GRP 78/BiP, and GRP 94 (35) were raised in rabbits using the procedure of Kreis (27) and affinity purified against the corresponding peptide. Characterization of these antibodies will be reported elsewhere (Fuller S. D., and J. Tooze, manuscript in preparation).

Antiserum was also raised in a rabbit against the content of isolated guinea pig zymogen granules. By immunoblotting guinea pig zymogen granule content (the immunogen), separated by two-dimensional gel electrophoresis by the procedure of Scheele and Palade (47), we established that this antiserum contained antibodies against all of the guinea pig zymogens with the exception of RNase (data not shown). We also raised an antiserum in a rabbit against rat pancreatic juice collected by catheterization of the pancreatic duct. By immunoblotting two-dimensional gels of rat pancreatic juice, we established that it contains antibodies against all of the rat zymogens (not shown); we also established that these antibodies against rat zymogens cross-reacted with most guinea pig zymogens, the notable exception being guinea pig amylase (not shown).

Using individual zymogens separated by SDS-PAGE and transferred to nitrocellulose, we affinity purified from both of these antisera antibodies specific for individual zymogens of the rat and guinea pig. Their monospecificity was established by immunoblotting zymogens separated by two-dimensional gel electrophoresis. We are also very grateful to Dr. H. Geuze (University of Utrecht, Utrecht, Netherlands) for generously providing a rabbit antibody against bovine chymotrypsinogen.

Electron Microscopy

For conventional electron microscopy, freshly dissected pancreatic lobules were fixed at room temperature for 1 h in 2–4% glutaraldehyde and 2% formaldehyde in 0.1 M sodium cacodylate buffer, pH 7.2. They were then given three 10-min washes in 0.1 M sodium cacodylate buffer, pH 7.2, and postfixed in 2% OsO_4 in 0.1 M cacodylate buffer, pH 7.2, for 1 h. After three additional washes in the buffer, the tissue was incubated overnight at 4°C in 0.5% magnesium uranyl acetate (BDH Chemicals Ltd., Poole, England) in water. It was then dehydrated in ethanol and embedded in Epon.

For cryoimmunoelectron microscopy, fresh pancreatic lobules were fixed for 15–20 min at 4°C in 3% paraformaldehyde in Mg^{++} - and Ca^{++} -free PBS and then transferred into 8% paraformaldehyde in PBS at room temperature for at least 1 h. They were then washed in PBS, infiltrated with sucrose, and frozen in liquid nitrogen; thin sections of frozen cells were cut and labeled according to published procedures (21, 51).

3-C2,4-Dinitroanilino-3'-amino-N-methylpropylamine (DAMP) Labeling

We followed published procedures (1, 2) and used immunogold labeling to detect the DAMP. We are grateful to R. G. W. Anderson (University of Texas Health Sciences Center, Dallas, TX) for generously giving us DAMP and anti-DAMP antibody.

Image Processing

Quasi-optical filtering and correlation averaging of crystalline areas were performed with the SEMPER image processing system (Image Processing Techniques of Cambridge Ltd., Cambridge, UK) after densitometry with an Optronics drum scanner at a 25- μm step size.

Results

Induction of ICGs in Guinea Pig Pancreas

ICGs were seen in <1% of the exocrine cells of pancreas from healthy guinea pigs that had free access to food and wa-

of tubules of RER. (C) Lysosomal compartments (arrow) accumulate DAMP as is shown by immunogold labeling of cryothin sections with antibody against DAMP. The neighboring RER cisternae with ICGs (arrowheads) are unlabeled, indicating that they are not acidic. Bars, 0.5 μm .

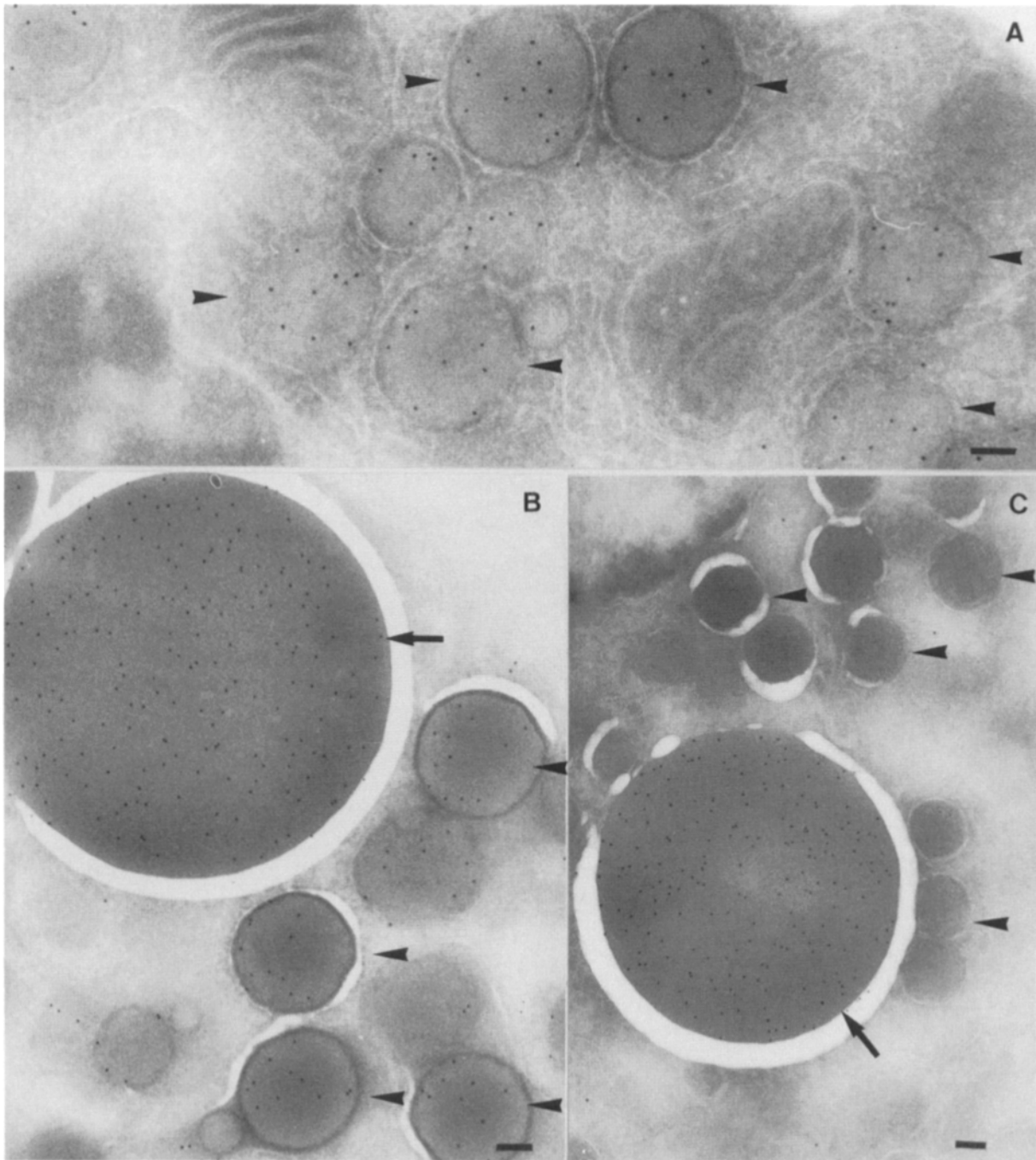


Figure 2. ICGs contain chymotrypsinogen. (A) Antibody against bovine chymotrypsinogen labels zymogen granules (not shown) and ICGs in cryothin sections (*arrowheads*). (B) Antibody against rat chymotrypsinogen also labels ICGs (*arrowheads*) and zymogen granules (*arrow*). (C) Antibody against rat pancreatic lipase labels zymogen granules (*arrow*) but does not label ICGs (*arrowheads*). Bars, 0.1 μm .

ter. Starvation and refeeding usually resulted in a significant increase in both the number of cells containing ICGs and the number of ICGs per cell. In some animals ICGs occurred in $\sim 30\text{--}50\%$ of the cells, as judged by electron microscopy. Although there was a variation between individual guinea pigs, injection of CoCl_2 usually induced very large numbers of ICGs in 80–95% of the exocrine cells. ICGs occurred throughout the endoplasmic reticulum (Fig. 1), and their presence in a cell correlated with a great reduction in the

number of post-Golgi zymogen granules. The largest ICGs had a diameter less than half the average diameter of zymogen granules (see Fig. 2). Since the endoplasmic reticulum can dilate to accommodate clusters of ICGs (Fig. 1), it is unlikely that their relatively small size and great number is a result of inelasticity of the cisternal membrane. Rather it appears that induction leads to myriads of nucleation events each resulting in an individual ICG. We found no morphological evidence to suggest that ICGs fuse.

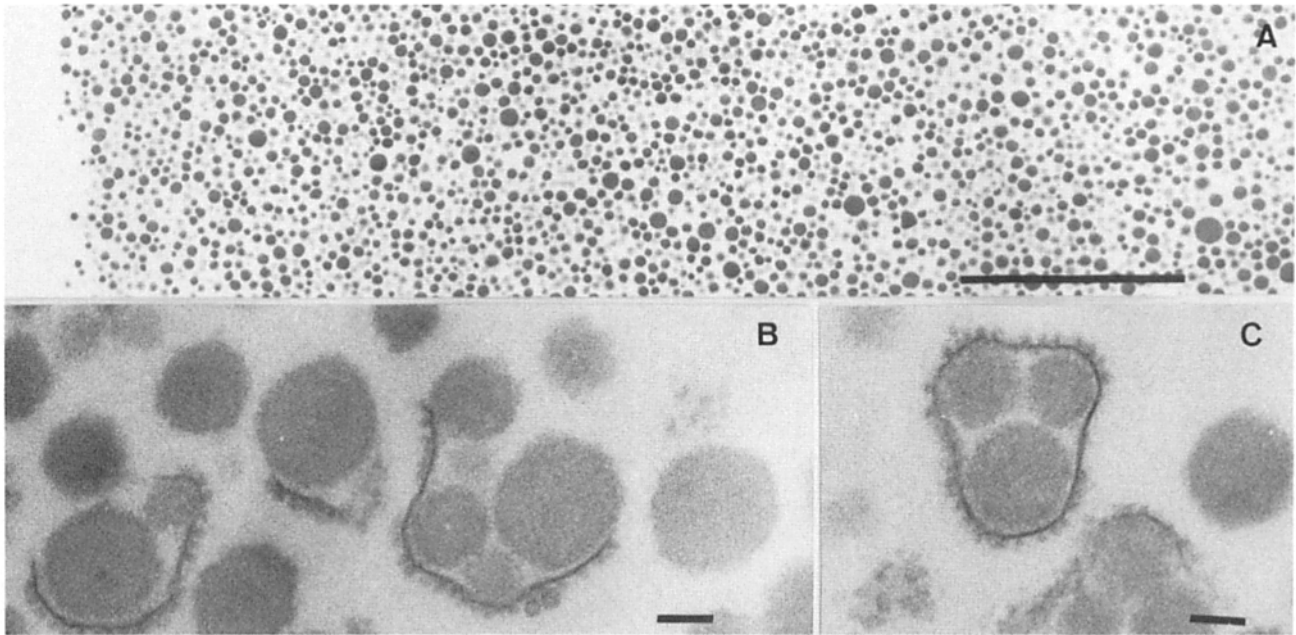


Figure 3. Morphology of isolated ICGs. (A) An electron micrograph of a section through the entire pellet of the ICG fraction. Note the remarkably homogeneous composition. The vast majority of the ICGs were liberated from the RER by the homogenization. B and C show examples of the minority which were either partially or completely enclosed in RER membrane. Mitochondria and zymogen granules were not observed within the ICG fractions. Bars: (A) 5 μm ; (B and C) 0.1 μm .

RER Containing ICGs Is Not Acidic

The endoplasmic reticulum is not an acidic compartment. To establish that the induction of ICGs is not accompanied by, or dependent upon, an acidification of the RER, we induced ICGs, and then isolated pancreatic lobules and labeled them *in vitro* with DAMP (2). Compartments that had accumulated DAMP were then revealed in cryosections using the protein A-gold technique. The RER was not labeled in cells either lacking or containing ICGs. Lysosomal compartments close to the RER containing ICGs were, however, labeled (Fig. 1); in addition, *trans* Golgi condensing vacuoles were heavily labeled with DAMP (not shown), as reported (36). Clearly the condensation of zymogens into ICGs in the RER occurs at a neutral pH.

ICGs Contain the Entire Complement of Zymogens

The zymogens account for >90% of the proteins synthesized in exocrine pancreatic cells (10). One can therefore argue *a priori* that ICGs must contain zymogens because they are the only proteins present in the lumen of the RER in amounts sufficient to give rise to so many granules. To directly establish that the ICGs contain all the zymogens, we adopted two approaches—immunocytochemistry and cell fractionation.

Immunocytochemical Evidence

Using an antibody against bovine chymotrypsinogen, we confirmed by immunogold labeling that ICGs contain this zymogen (Fig. 2), as reported (20). We could also label ICGs, as well as condensing vacuoles and zymogen granules, with a rabbit antiserum against rat pancreatic juice (not shown). We affinity purified from the latter antiserum antibodies specific for different rat zymogens. All of these specific antibodies labeled zymogen granules and condensing

vacuoles in cryosections of both rat and guinea pig pancreas (Fig. 2). However, only the affinity-purified antibody specific for rat and guinea pig chymotrypsinogen labeled guinea pig ICGs (Fig. 2). These labeling results were the same regardless of whether the ICGs had been induced by Co^{++} or by starvation and refeeding. They established that ICGs contain chymotrypsinogen, but they failed to provide evidence for the presence of any of the other zymogens. We therefore isolated ICGs and biochemically analyzed their composition.

Biochemical Evidence

Using sucrose gradient centrifugation, ICGs were isolated from the pancreas of guinea pigs injected with CoCl_2 . Electron microscopy of the same pancreas (not shown) confirmed that there had been a massive induction of ICGs. The ICG fraction was shown to be homogeneous by electron microscopy: it comprised free ICGs and a minor component of ICGs partially or completely surrounded by RER membrane (Fig. 3). There were very few RER vesicles without ICGs, and other organelles, including zymogen granules, were not observed.

Aliquots of the ICG fraction were dissolved in sample buffer under reducing and nonreducing conditions, and analyzed by SDS-PAGE followed by Coomassie blue staining or immunoblotting. A zymogen granule fraction from normal guinea pigs was analyzed in parallel. Fig. 4 shows a typical result. Under both nonreducing and reducing conditions, isolated zymogen granules were completely solubilized in sample buffer containing 2% SDS. Electrophoresis followed by Coomassie blue staining revealed the entire complement of zymogens. The electrophoretic mobilities of guinea pig zymogens change significantly upon reduction(46), indicat-

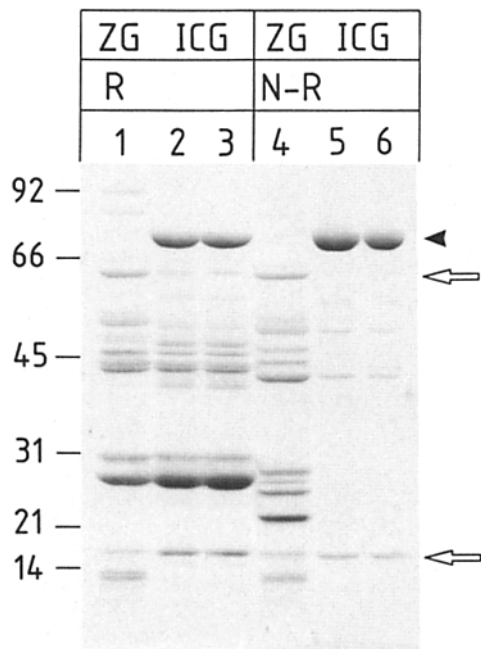


Figure 4. Coomassie blue-stained SDS-polyacrylamide gel of guinea pig zymogen granules and ICGs. Lane 1 shows zymogen granule content solubilized under reducing conditions. Lanes 2 and 3 show ICG fractions solubilized under the same reducing conditions. Note that the ICGs contain the zymogens present in zymogen granules (bands between the arrows). The identification of these proteins as zymogens was shown by immunoblotting (see Fig. 5). Lane 4 shows zymogen granule content solubilized under nonreducing conditions. Compare lane 4 with lane 1; these proteins have different mobilities after reduction and acetylation. Lanes 5 and 6 show proteins solubilized from ICGs under nonreducing conditions. Most of the zymogens were insoluble, except RNase (*lower arrow*) and traces of some of the higher molecular mass zymogens. Note under both reducing and nonreducing conditions an abundant protein of 78 kD is solubilized from ICGs (*arrowhead*); this protein, which is not present in zymogen granules (see lanes 1 and 4), was identified as GRP 78/BiP by specific antibodies (see below). The bands at ~13 kD in the zymogen granule fraction did not react with any of our antizymogen antibodies. The positions to which molecular mass markers migrate are shown at the left.

ing the presence of extensive intramolecular disulphide bonding (Fig. 4, lanes 1 and 4).

The ICG fraction was also readily soluble under reducing conditions, and the stained gels revealed the presence of the full complement of zymogens (Fig. 4, lanes 2 and 3). Immunoblotting with antiserum against guinea pig zymogens (Fig. 5) and rat zymogens (not shown) confirmed the results of Coomassie blue staining. The ICGs, like the zymogen granules, contained RNase, chymotrypsinogen, trypsinogen, the procarboxypeptidases, proelastases, amylase, and lipases. This confirmed that the ICGs are indeed coaggregates of the entire set of zymogens.

By contrast, under nonreducing conditions the ICGs did not dissolve; very little zymogen protein was separated on the gel (Fig. 4, lanes 5 and 6), but material was present in the stacking gel (not shown). Four sequential attempts to solubilize ICGs in nonreducing sample buffer containing 2% SDS were carried out (Fig. 6, lanes 3-6), and each time a large insoluble pellet remained. This pellet was solubilized

only under reducing conditions, and SDS-PAGE showed that it contained most of the zymogens (Fig. 6, lane 7). Of the complement of zymogens, only RNase was soluble in significant amounts under nonreducing conditions (Fig. 6, lanes 3-6). In ICGs the zymogens must, therefore, be cross-linked by intermolecular disulphide bonds into insoluble aggregates, except about half of the RNase and traces of some of the higher molecular mass molecules. This may explain our puzzling immunocytochemical results. Misfolding and extensive intermolecular disulphide bonding of the zymogens apparently obscures epitopes recognized by our antibodies, with the exception of one or more epitopes of chymotrypsinogen. However, the immunocytochemical and biochemical data combined indicate that the ICGs contain the complete set of zymogens.

ICGs Exclude PDI and GRP 78/BiP

PDI and GRP 78/BiP are abundant soluble resident proteins of the RER (34, 35, 39). In exocrine pancreatic cells PDI and GRP 78/BiP occur in solution with zymogens in the RER. If condensation of zymogens into ICGs at neutral pH is a sorting event, both PDI and GRP 78/BiP should be excluded. As will be described elsewhere (Fuller, S. D., and J. Tooze, manuscript in preparation), antibodies have been raised in rabbits against PDI purified from rat liver microsomes. In addition, antibodies were raised against synthetic peptides corresponding to the carboxy-terminal sequences of PDI and GRP78/BiP. Immunoblots showed that these three antibodies react specifically with their respective proteins from rat and guinea pig pancreas. They were used to label ICGs, which had been induced by starvation and refeeding or with CoCl_2 in the guinea pig pancreas.

As Fig. 7 shows, the two PDI antibodies and the GRP 78/BiP antibody labeled the lumen of the RER; luminal labeling was especially striking in sections of distended cisternae containing ICGs. The perimeter of the ICGs was labeled, but the interior of these granules was unlabeled by all three antibodies. It should be borne in mind that the gold particles used for immunolabeling can be as much as 150 Å from the antigen. Clearly GRP 78/BiP and PDI are excluded from the interior of the ICGs.

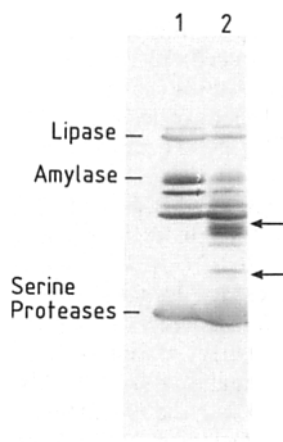


Figure 5. Immunoblots of zymogen granule and ICG content. Zymogen granules and ICGs were solubilized under the same reducing conditions. The proteins were separated by SDS-PAGE, transferred to nitrocellulose, reacted with antiserum against guinea pig zymogen granule content, and detected with anti-rabbit IgG peroxidase. Comparison of lane 1 (zymogen granules) with 2 (ICGs) shows that they contain the same zymogens. In addition, the ICGs contain immunoreactive proteins not present in the zymogen granules (bands between the arrows).

As the Coomassie blue staining of ICG content shows (Fig. 4, lanes 2 and 3), these proteins are not abundant. We assume they are fragments of the higher molecular mass zymogens produced by partial proteolysis.

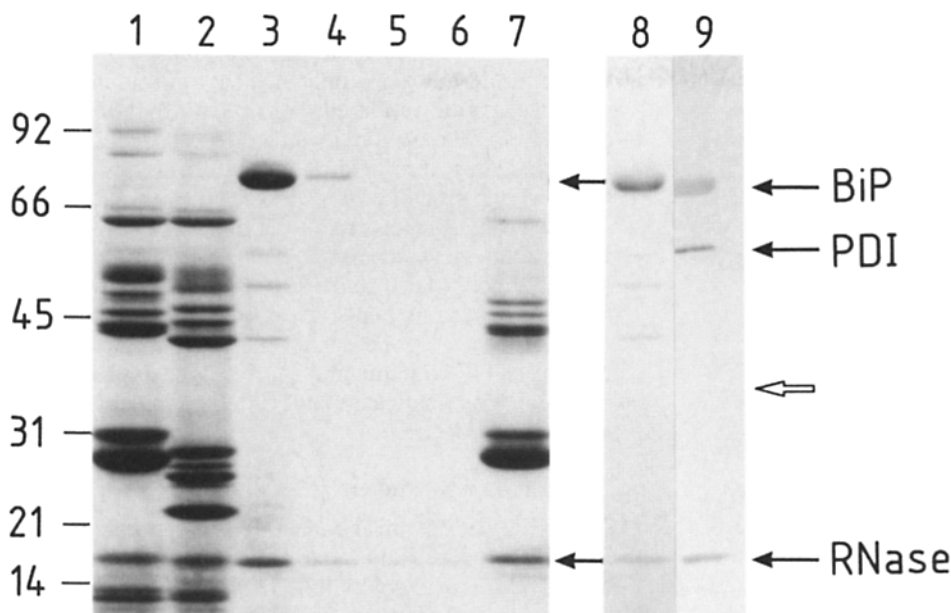


Figure 6. Coomassie blue staining of proteins eluted from ICGs under nonreducing conditions and their identification with specific antibodies. Lanes 1 and 2 show the content of zymogen granules solubilized under reducing and nonreducing conditions, respectively. Lanes 3–6 show the proteins solubilized from ICGs by four successive washings in non-reducing sample buffer containing 2% SDS. The major proteins eluted are GRP 78/BiP and RNase. Lane 7 shows the pellet of ICGs after four washings and subsequent solubilization under reducing conditions. Compare lane 7 with lane 1: the ICGs contain the complete set of zymogens but, with the exception of RNase, they can only be solubilized under reducing conditions. Lane 8 shows Ponceau S staining of proteins

eluted from isolated ICGs by washing in nonreducing sample buffer containing 2% SDS. Lane 9 shows an immunoblot of the gel. The 78-kD protein reacted with an antibody specific for GRP 78/BiP. An antibody specific for PDI labeled a 56-kD band barely visible by Ponceau S staining. An antibody specific for RNase labeled a band with an apparent molecular mass of 17 kD. The nitrocellulose filter was cut in half before blotting (arrow), and the upper half was sequentially blotted with antibodies against GRP 78/BiP and PDI. The lower half was blotted with antibody against RNase. The positions of molecular mass markers are indicated on the left.

As described above (Figs. 4 and 6), attempts to solubilize isolated ICGs under nonreducing conditions in the presence of 2% SDS released very little protein. Most of the zymogens remained insoluble in granular form. Analysis by immunoblotting of the proteins solubilized from the ICGs under nonreducing conditions (Fig. 6, lanes 8 and 9) established the following: the abundant 78-kD protein, which was not present in zymogen granules, proved to be GRP 78/BiP. The protein with an apparent molecular mass of 17 kD, which was also present in zymogen granules, was RNase. A minor soluble protein with an apparent molecular mass of ~56 kD proved to be PDI. In addition, trace amounts of some other zymogens could be detected by blotting (not shown). We also found that almost all of the GRP 78/BiP, but none of the RNase, could be dissolved from ICGs by 10 mM Mg ATP in PBS (Fig. 8). We interpret this to mean that RNase is within the granule core and can only be released by detergent, whereas GRP 78/BiP is at the surface of the ICGs and can be solubilized in the absence of detergent. ATP is known to dissociate GRP 78/BiP from its complexes with misfolded proteins (24, 34).

Finally we fixed and embedded unwashed ICGs and ICGs that had been washed four times with nonreducing gel sample buffer to solubilize all the GRP 78/BiP (Fig. 6), and then labeled cryosections with antibodies against GRP 78/BiP, PDI, and chymotrypsinogen. GRP 78/BiP antibodies labeled the surface of unwashed ICGs but not their interior, whereas the washed ICGs were completely unlabeled (Fig. 9). The same pattern of labeling was obtained with the PDI antibody (not shown). By contrast, chymotrypsinogen antibody labeled unwashed (not shown) and washed ICGs (Fig. 9), and this labeling was not restricted to the granules' surface.

Combining the immunocytochemical and biochemical data we conclude that (a) GRP 78/BiP and PDI are associated

with the surface layer of ICGs, but both are excluded from the interior of the granules; (b) GRP 78/BiP and PDI are not disulphide bonded to the cross-linked zymogens; and (c) the amount of GRP 78/BiP associated with the surface of the isolated ICGs is much greater than the amount of PDI (Figs. 4 and 6).

Coordinate Induction of PDI, GRP 78/BiP, and GRP 94

The accumulation of misfolded proteins in the RER induces the synthesis of GRP 78/BiP and GRP 94 (26). ICGs are aggregates of massive amounts of misfolded proteins; their presence should therefore be a potent signal for the induction of GRP 78/BiP and GRP 94. To test this, we prepared lobules from pancreas containing ICGs induced with CoCl_2 and from normal pancreas as a control. The lobules were then incubated from 15 to 60 min in medium containing [^{35}S]cysteine and [^{35}S]methionine, and then the labeled proteins were analyzed by SDS-PAGE. As Fig. 10 A shows, the synthesis of the zymogens was virtually identical in the control and experimental lobules, indicating that massive induction of ICGs by CoCl_2 does not inhibit protein synthesis. In addition, the relative rates of synthesis of the individual enzymes remain unchanged. However, as Fig. 10 A also shows, significantly more label was incorporated into bands with apparent molecular masses of 56, 78, and 94 kD in the lobules containing ICGs than in the control. The 56- and 78-kD bands were positively identified as PDI and GRP 78/BiP by immunoblotting with our antibodies specific for these two proteins (Fig. 10 A). In addition, we confirmed the induction of PDI by immunoprecipitation of this protein from the pancreatic cell extracts with our antibody against rat PDI (Fig. 10 B). GRP 94 was identified by immunoblotting with a rabbit antiserum raised against its carboxy terminus (Fig. 10 A).

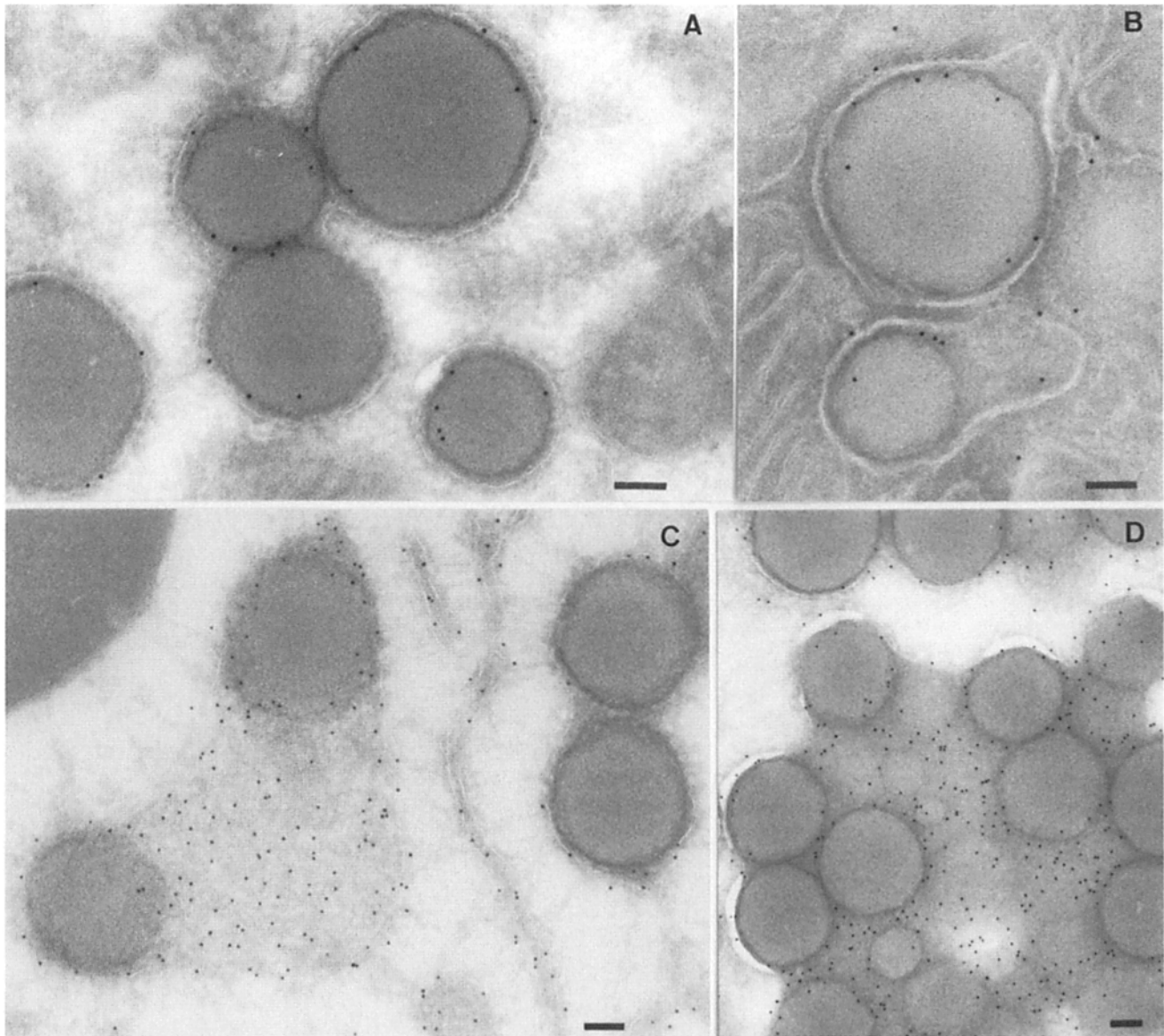


Figure 7. ICGs exclude GRP 78/BiP and PDI. *A* and *B* are micrographs of cryosections of RER containing ICGs that had been immunogold labeled with an affinity-purified antibody specific for GRP 78/BiP. The labeling was restricted to the perimeter of the ICGs and the lumen of the RER. The interior of the ICGs was completely unlabeled. *C* and *D* show similar sections labeled with antibody specific for PDI: in *C* rabbit antibody against PDI from rat liver was used, and in *D* affinity-purified rabbit antibody against the carboxy-terminal peptide of PDI was used. The interior of the ICGs was again unlabeled while the granules' perimeter and the lumen of the RER were labeled. Note the distended cisterna with ICGs in *C* and *D* and compare them with the section of Epon-embedded material shown in Fig. 1 *A*. Bars, 0.1 μm .

To estimate the extent of the induction seen in Fig. 10, we measured, by slicing and counting gel bands, the amount of [^{35}S]cysteine and [^{35}S]methionine incorporated during 60 min into these three proteins and into RNase in control and experimental lobules. RNase was selected as a standard because incorporation into it was linear during the 60-min incubation. Moreover, in both experimental and control lobules the amount of label incorporated into RNase per 100 μg total protein was approximately the same. We found that synthesis of PDI, GRP 78/BiP, and GRP 94 was induced on average 2.5-, 3-, and 4-fold more, respectively, in pancreas containing ICGs compared to normal pancreas. These data establish unequivocally that in this system PDI synthesis is

induced coordinately with the induction of GRP 78/BiP and GRP 94.

Effect of Co^{++} on Pancreatic Cell Metabolism

To assess the effect of cobalt ions on the metabolism of guinea pig pancreatic cells, in the hope of finding clues as to the mechanism of induction of ICGs, we prepared lobules from normal pancreas and incubated them in media containing different concentrations of Co^{++} . Over the 10^{-3} – 10^{-4} M range, Co^{++} had no detectable effect on total protein synthesis (Fig. 11 *A*). However, over the 10^{-2} – 10^{-5} M range, Co^{++} inhibited cellular respiration in a dose-dependent manner

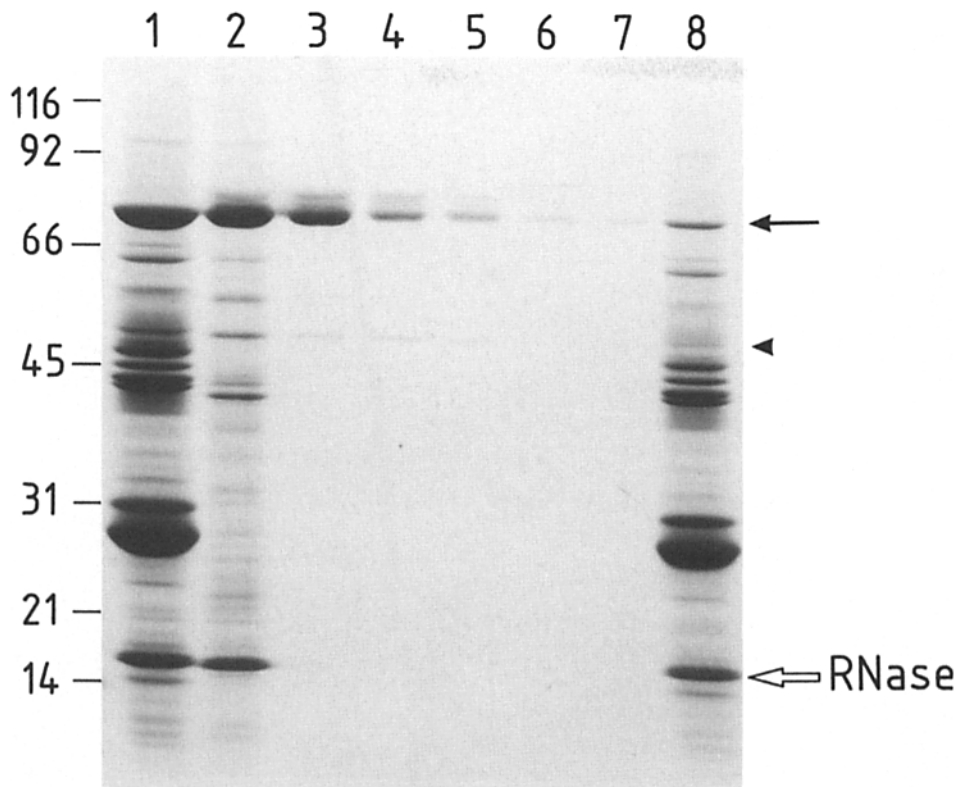


Figure 8. Coomassie blue staining of proteins eluted from ICGs by 10 mM Mg ATP. Lanes 1 and 2 show ICGs dissolved under, respectively, reducing and non-reducing conditions both in the presence of 2% SDS. Lanes 3–7 show that five consecutive washes of ICGs in PBS containing 10 mM Mg ATP, but no detergent, solubilizes only GRP 78/BiP (arrow) and an unidentified protein (arrowhead). Lane 8 shows the pellet of ICGs after the five washes in Mg ATP and subsequent solubilization under reducing conditions. Note that RNase (open arrow) is not solubilized from ICGs under nonreducing conditions in the absence of 2% SDS. The additional minor bands seen in lanes 1, 2, and 8, which are not visible in Fig. 4, lanes 2, 3, 5, and 6), are degradation products of zymogens, which are more obvious because the gel shown in Fig. 8 was much more heavily loaded than that shown in Fig. 4. The positions of molecular mass markers are shown at the left.

(Fig. 11 B). Furthermore, in a pulse-chase protocol Co^{++} at 10^{-3} and 10^{-4} M significantly inhibited the movement of labeled zymogens from the RER into post-Golgi zymogen granules (Fig. 11 B). In short, at 10^{-3} M Co^{++} protein synthesis was normal, but both cellular respiration and transport of pulse-labeled zymogens from the RER to zymogen granules was $>50\%$ inhibited. Apparently in these cells protein transport is more sensitive to reduction in ATP levels than protein synthesis, and this may be the basic mechanism for the induction of ICGs.

Finally, we incubated for periods of up to 3 h lobules from normal guinea pig pancreas in media containing [^{35}S]methionine and cysteine and either no Co^{++} or 10^{-2} or 10^{-3} M

Co^{++} . The labeled zymogens were then analyzed by SDS-PAGE under reducing and nonreducing conditions. In the nonreducing gels there was no evidence of intermolecular cross-linking, and aggregation of the labeled zymogens was made in the presence of Co^{++} at these two concentrations (data not shown) over a 3-h period. Hence we can conclude that Co^{++} at these concentrations did not inhibit the enzymatic activity of PDI.

Crystals in Rat Pancreas

Within a day of injecting 50 mg/100 g body weight of parachlorophenylalanine methylester into the peritoneum of rats,

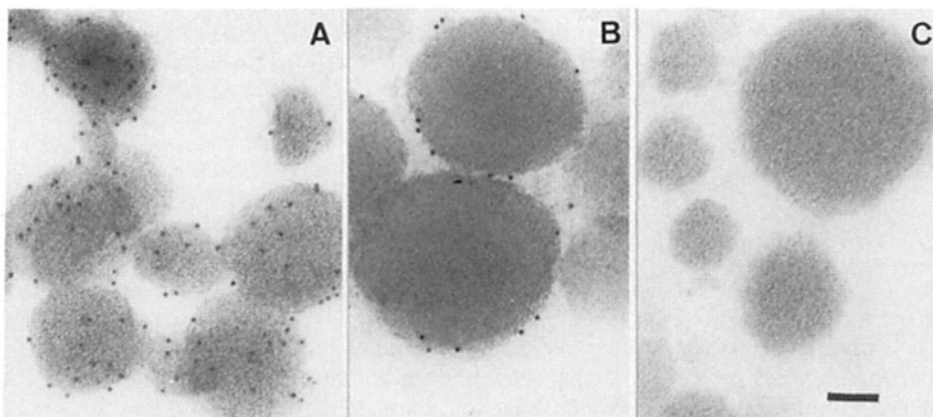


Figure 9. Immunolabeling of isolated ICGs. (A) Isolated ICGs, washed four times in buffer containing 2% SDS and then fixed and sectioned, were labeled by antibody against chymotrypsinogen. The same result was obtained with unwashed ICGs (not shown). Note that the immunogold labeling is over the whole surface of the sectioned granules. (B and C) The perimeter of isolated ICGs, fixed and sectioned without washing in buffered 2% SDS, was immunogold labeled by affinity-purified antibody specific for GRP 78/BiP. Note that there

was no labeling of the interior of the granules. (D) After four washes in buffered 2% SDS, ICGs could not be labeled by antibody against GRP 78/BiP. The same pattern of labeling was obtained with antibody against PDI (not shown). Bars, 0.1 μm .

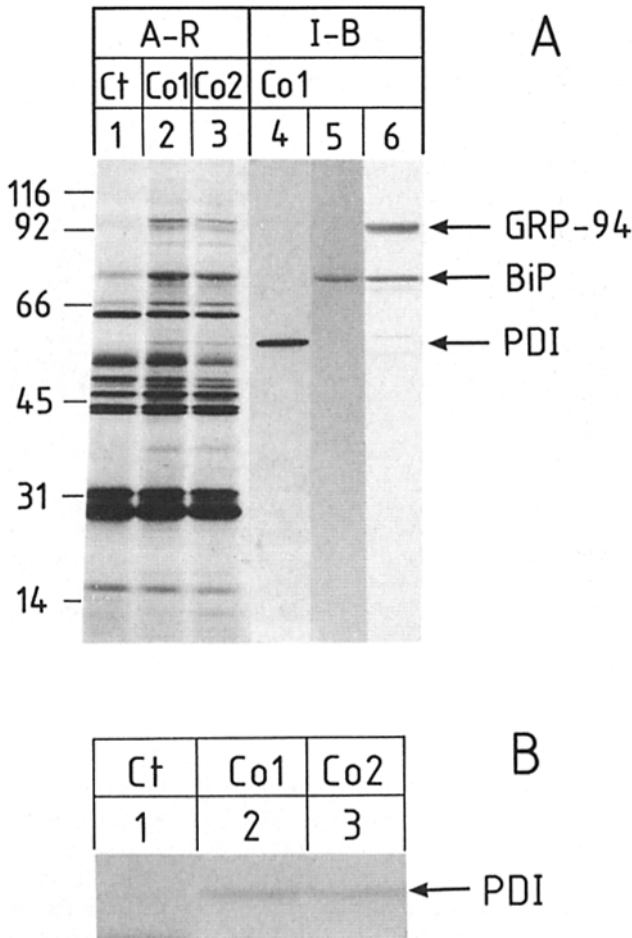


Figure 10. Coordinate induction of the synthesis of GRP 94, GRP 78/BiP, and PDI. (A) Pancreatic lobules were prepared from a normal guinea pig and two guinea pigs injected with CoCl_2 to induce ICGs. The lobules were incubated at 37°C with oxygenation for 1 h in the presence of ^{35}S methionine and ^{35}S cysteine. They were then homogenized, and the proteins were dissolved under reducing conditions. After SDS-PAGE, the incorporation of label into individual proteins was visualized by fluorography. Lane 1 shows normal control pancreas; lanes 2 and 3 show pancreas with ICGs from two different guinea pigs (Co1 and Co2) injected with CoCl_2 . Lanes 4-6 show the Co1 sample immunoblotted with our antibodies. The arrows point to PDI, GRP 78/BiP, and GRP 94, whose synthesis is coordinately induced in the experimental lobules. Additional bands at ~ 105 , 85, 40, and 17 kD are also induced, but we have not identified these proteins. The position of the molecular mass markers is shown at the left. (B) PDI was immunoprecipitated from 1 mg protein of the control and two experimental samples using a polyclonal antibody that is specific for PDI and then subjected to SDS-PAGE. The fluorograph is shown. This result confirms that the 56-kD protein, whose synthesis is induced (A), is indeed PDI.

crystals form in the RER cisternae of pancreatic exocrine cells (5, 17). Electron microscopy of conventionally fixed and embedded pancreas revealed the crystals running for many micrometers inside many of the cisternae (Fig. 12 A); as a result, the cisternae were closely packed into parallel arrays. When the crystals were longitudinally sectioned, the close apposition of the cisternal membrane to the crystal was

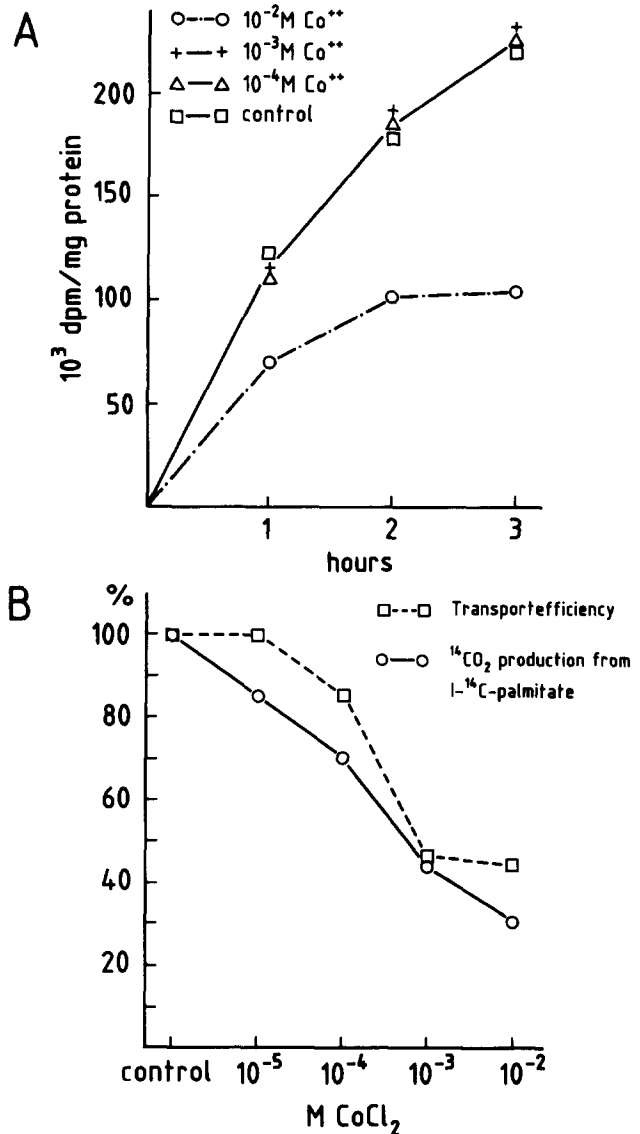


Figure 11. Effect of Co^{++} on synthesis, transport, and respiration in isolated guinea pig pancreatic lobules. A shows that 10^{-3} and 10^{-4} M Co^{++} had no effect on the incorporation of ^3H leucine into total pancreatic proteins. 10^{-2} M Co^{++} inhibited protein synthesis by $\sim 50\%$. (B) The open circles show the linear dose-dependent decrease in cellular respiration caused by Co^{++} , as determined by the production of $^{14}\text{CO}_2$ from ^{14}C -labeled palmitate. The open squares show the effect of Co^{++} on the transport of pulse-labeled zymogens from RER into zymogen granules as determined by cell fractionation. Comparison of A with B demonstrates that at 10^{-3} M Co^{++} , total protein synthesis is not different from controls, whereas respiration and transport of radiolabeled zymogens are $>50\%$ inhibited. All data points in A and B are the average of at least five determinations; the standard deviation from the mean was always $<10\%$. In this figure, transport efficiency is defined as the amount of 5-min pulse-labeled protein reaching the zymogen granule fraction in 60 min of chase and normalized to 100% in control lobules.

clearly revealed (Fig. 12 B). It is noteworthy that where the crystals end, the cisternal membranes tend to diverge (Fig. 12 C).

We wished to determine whether individual crystals contained only one species of zymogen or several different zymo-

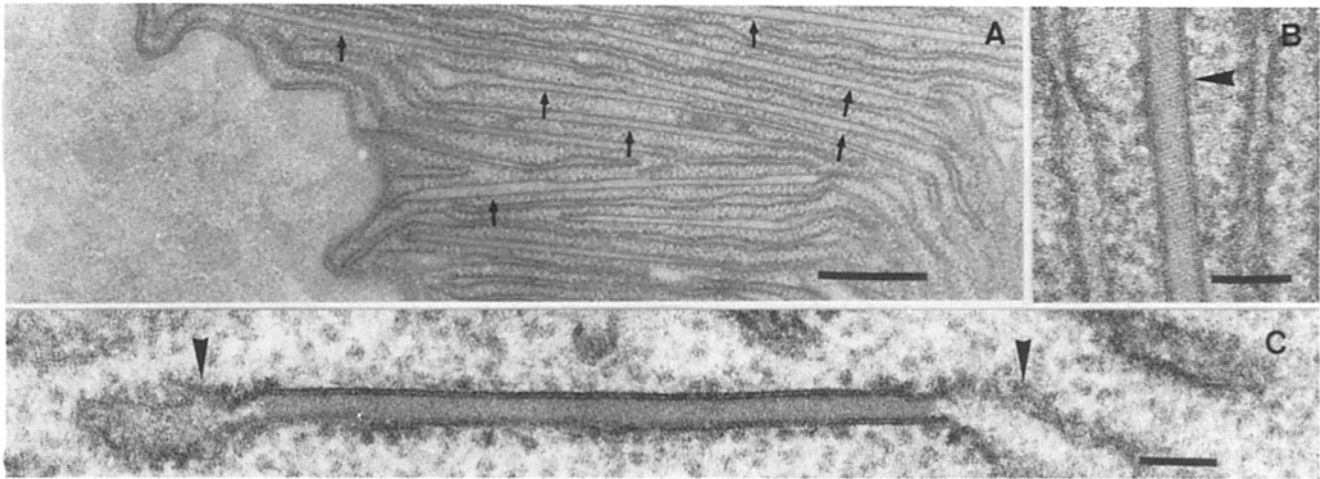


Figure 12. Crystals in rat pancreas. Conventional electron microscopy revealed crystals within the lumen of the RER of rat exocrine pancreatic cells, after injection of the animals with parachlorophenylalanine methylester. *A* shows that the crystals (*arrows*) remain in the plane of the thin sections for many micrometers. The crystals must be rigid because they deform the cisternae, constraining them into parallel arrays. *B* shows that the crystals (*arrowhead*) fill the lumen of the RER, leaving no space between the crystal surface and the inner face of the RER membrane. *C* shows that where the crystals terminate, the cisternal membranes diverge and the lumen is dilated (*arrowheads*). Bars: (*A*) 0.5 μm ; (*B* and *C*) 0.1 μm .

gens. An antiserum raised against total rat exocrine pancreas secretion, obtained from the pancreatic duct, was affinity purified on six different zymogens. The antiserum against the total pancreatic secretion heavily labeled the crystals in cryothin sections (not shown). The results with the six affinity-purified antibodies (Fig. 13) can be summarized as follows: (*a*) all six antibodies—antiamylase, antilipase, anticarboxy peptidase, antitrypsinogen, antichymotrypsinogen, and antiRNase—labeled at least some of the crystals in each field examined; (*b*) antiamylase, antilipase, and antichymotrypsinogen antibodies labeled all of the crystals; (*c*) antiamylase labeled the crystals much more heavily than any of the other antibodies, with antilipase and antichymotrypsinogen giving the next heaviest labeling; and (*d*) using three antibodies—antiamylase, antilipase, and antichymotrypsinogen—in pairwise combinations in a double-labeling protocol with 5- and 9-nm gold particles, we could show directly that the crystals contained these three zymogens, amylase being preponderant. Taken together these results indicate that all six zymogens tested occur within the crystals, albeit in very different amounts. The major component of the crystals is amylase; in rat pancreas the two isoforms of amylase constitute at least 30%, and probably closer to 50%, of the total zymogens synthesized (42, 48).

Fine Structure of Zymogen Crystals

Visual comparison of the images of the crystals in Epon-embedded material and in cryosections (Figs. 12 and 13) indicated that the fine structure was much better preserved in the latter. Tilting of obliquely sectioned crystals with a non-orthogonal pattern produced characteristic orthogonal patterns, indicating that all the observed views resulted from the same crystal (not shown). Analysis of the optical diffraction of these crystals is consistent with a unit cell of $a \approx b \approx 35 \text{ \AA}$, $c \approx 75 \text{ \AA}$, $\alpha \approx \beta \approx \gamma \approx 90^\circ$ or $80,000 \text{ \AA}^3$. This unit cell

is presumably a low estimate, since the fixation, sectioning, and staining should cause some shrinkage. Quasioptical filtering and correlation averaging of crystalline areas reveal a bilobed density (Fig. 13 *F*). We suggest that these crystals are of amylase; it is the most abundant zymogen in the rat pancreas, it crystallizes readily (12) in an orthorhombic space group (32), and it has the appropriate size and shape to be the bilobed density seen in filtered or correlation-averaged images (38). The analysis of these crystals was complicated by the negative staining used to enhance the contrast of the cryothin sections and by the frequent presence of edge dislocations. These dislocations were most clearly seen in sections parallel to the axis and appeared to separate the crystals into layered domains. Since the crystalline regions are primarily amylase, but also include all the other zymogens, the observed dislocations could easily represent the sites of inclusion of the other proteins between the crystalline amylase layers.

Amylase contains four intramolecular disulphide bonds as well as two free sulphhydryls. Therefore, we investigated the solubility of these crystals to see whether the amylase molecules were cross-linked by intermolecular disulphide bonds, as is the case with the zymogens in ICGs, or whether the organization of the amylase molecules in the crystals prevented their cross-linking. Phase-contrast microscopy of crystals in subcellular fractions indicated that, in contrast to isolated ICGs, they were rapidly solubilized by treatment with 2% SDS in the absence of a reducing agent at room temperature. Furthermore, the crystals were dissolved by treatment with EDTA, which is consistent with the behavior of crystals of native amylase (32). These results and the fact that we were able to immunogold label six zymogens in the crystals (see above) indicate that all the proteins within the crystals are in their native conformation.

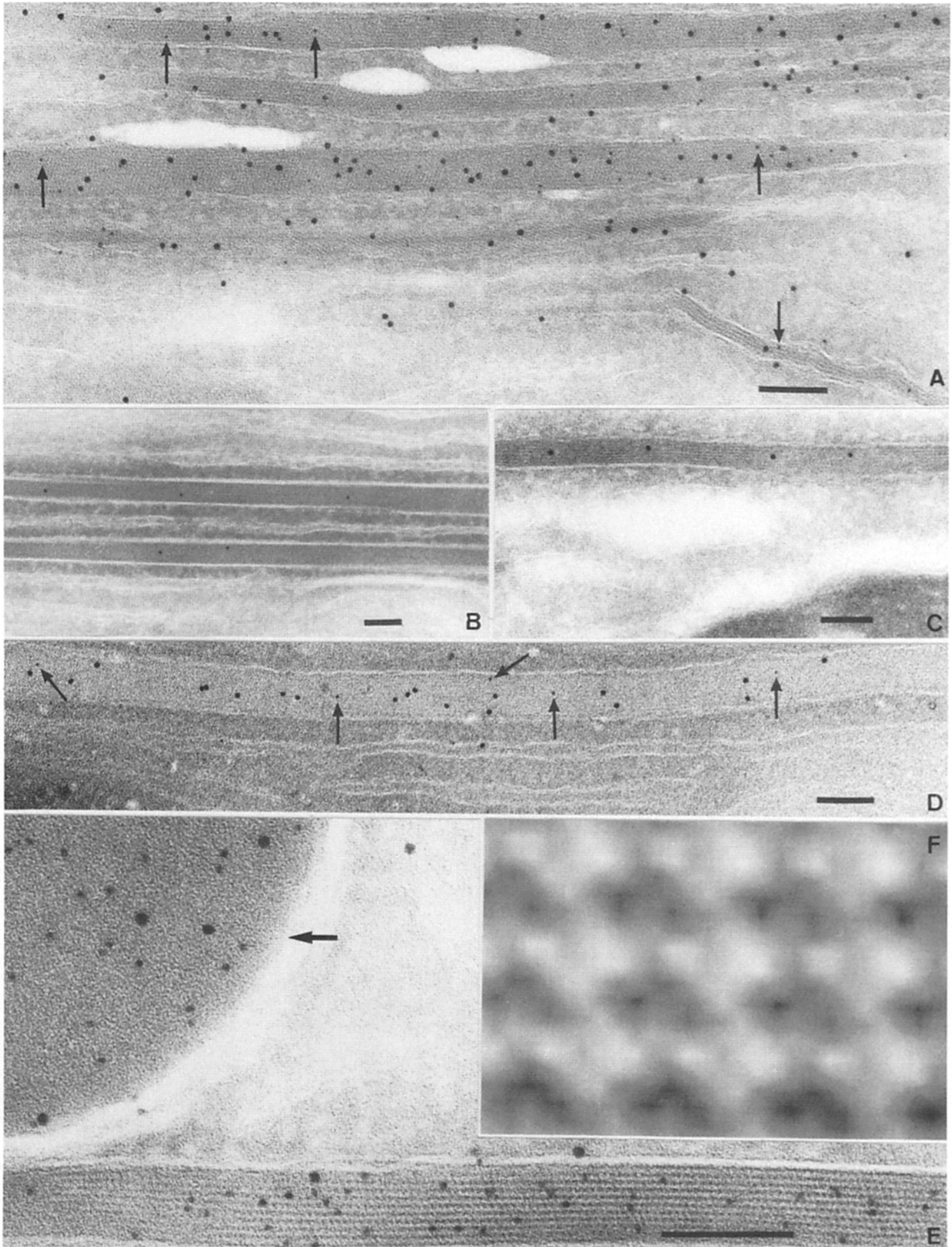


Figure 13. Crystals contain more than one zymogen. Cryosections of rat pancreatic cells containing crystals in the RER were immunogold labeled with anti-zymogen antibodies. *A* shows double labeling of crystals with antibodies against amylase (9-nm gold particles) and lipase (6-nm gold particles). Some of the 6-nm gold particles are indicated by arrows. *B* shows crystals labeled with antibody against chymotryp-

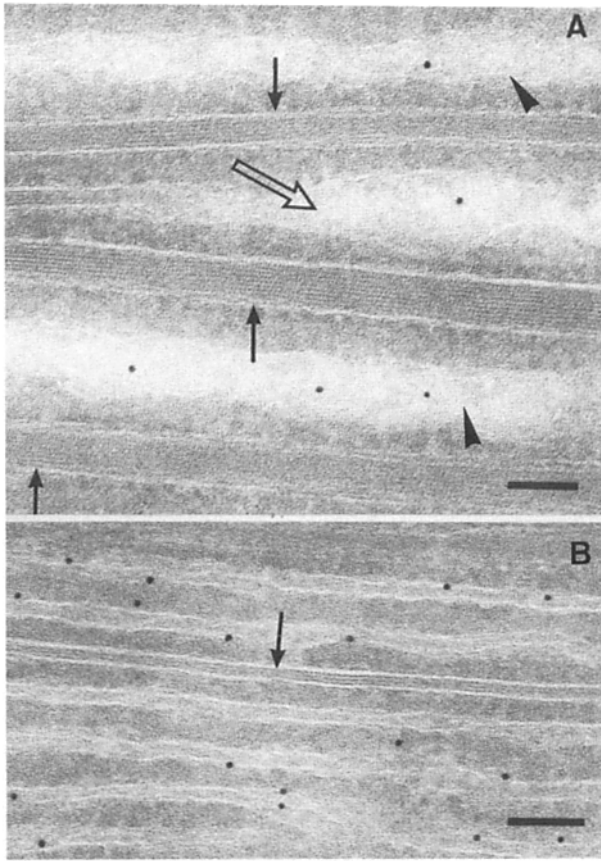


Figure 14. Zymogen crystals exclude PDI. Immunogold labeling of rat pancreas containing zymogen crystals with antibody against PDI. *A* shows that PDI is excluded from the crystals and the regions of the RER cisternae that contain them (*arrows*). Labeling is restricted to the lumina of cisternae without crystals (*arrowheads*). Note that where a crystal ends, labeling is seen in the cisternal lumen distal to it (*open arrows*). *B* shows one cisterna, with a crystal throughout its length (*arrows*), which is entirely unlabeled while all the other cisternae without crystals are labeled. The same pattern of labeling was obtained with antibody against GRP 78/BiP. Bars, 0.1 μm .

Zymogen Crystals Exclude GRP 78/BiP and PDI

Since the crystal structure is an amylase lattice with the other zymogens intercalated, we labeled cryosections of pancreas containing the crystals with our two antibodies against PDI and the antibody against GRP 78/BiP to determine whether or not these luminal RER proteins were also incorporated. None of these antibodies labeled any of the crystals (Fig. 14). All three of them labeled the lumina of RER cisternae that did not contain crystals. Labeling was not observed along the edges of crystals between the crystal surface and the closely applied inner face of the cisternal membrane. Clearly GRP

78/BiP and PDI are both excluded from the crystals and from adjacent regions of the cisternal membrane. After the administration of high doses of aromatic amino acids, total protein synthesis in pancreatic lobules *in vitro* was reduced <50% of controls. This precluded investigation of whether crystallization of native zymogens in the RER induces GRP 78/BiP and PDI synthesis.

Discussion

Formation of ICGs Is a Physiological Event

A few cells containing ICGs can usually be found in normal pancreas from healthy, well-fed, and watered guinea pigs. Starvation and refeeding, which must periodically happen to guinea pigs in the wild, not to mention children's pets, results in a striking increase in the number of cells with ICGs and the number of ICGs per cell (20, 37). The animals nevertheless survive and the ICGs are eventually depleted by autophagy (25, and our unpublished data). The formation and elimination of ICGs are, therefore, normal physiological events in the guinea pig. Furthermore, ICGs are not unique to guinea pigs; they have been observed in the pancreas of several other species including humans as well as in other exocrine and endocrine cells (20).

What Triggers ICG Formation

Starvation and refeeding or injections of Co^{++} induce the formation of ICGs which appear to be identical by morphological criteria. We did not isolate the ICGs induced by starvation and refeeding and have not directly proven that the zymogens they contain are cross-linked by intermolecular disulphide bonds. However, with our various antibodies against zymogens, the pattern of immunogold labeling of ICGs induced by starvation and refeeding is identical to that of ICGs induced by Co^{++} . We infer, therefore, that the ICGs are biochemically identical regardless of the method of induction.

These two methods of induction of ICGs are, we suggest, effective because they lead to an increase in the concentration of zymogens in the lumen of the RER that is sufficient to allow their *in situ* cocondensation. In cell-free systems, the export of proteins from the RER has been shown to be particularly sensitive to a reduction in the concentration of ATP (3), and our data on the effect of Co^{++} on the metabolism of pancreatic cells suggest the same is true *in vivo*. Since cellular respiration and movement of zymogens from the RER to zymogen granules are more sensitive to inhibition by Co^{++} than is zymogen synthesis, Co^{++} could result in an increase in the intraluminal concentration of the zymogens. It is significant that another manipulation which blocks cellular respiration (*i.e.*, incubating pancreatic cells under N_2 atmospheres) also induces ICGs (33), although not to the extent seen with Co^{++} injections. Refeeding after starvation

sinogen: *C* shows a crystal labeled with antibody against RNase. *D* shows a crystal double labeled with antibodies against amylase (9-nm gold particles) and chymotrypsinogen (6-nm gold particles, indicated by arrows). *E* shows part of a zymogen granule and a crystal labeled with antibodies against amylase (6-nm gold particles) and chymotrypsinogen (9-nm gold particles). Notice the crystal lattice which, as these figures show, varies in appearance depending on the angle of sectioning. *F* shows the quasi optical filtering of a section of an amylase crystal in the ER. The protein is light in this representation. Note the orthogonal unit cell containing a bilobed structure. Bars, 0.1 μm .

stimulates zymogen synthesis as well as secretion (our unpublished data) and might well lead locally in the RER of some cells to higher than normal concentrations of these proteins and hence to ICGs.

Formation of ICGs Is a Sorting Event

SDS-PAGE of isolated ICGs dissolved under reducing conditions establishes that these granules contain the complete set of zymogens. This finding, combined with the fact that in cryothin sections of ICGs—both in situ and after isolation—chymotrypsinogen antibodies label most of the granules, proves that individual ICGs are aggregates of more than one zymogen. The simplest interpretation of our finding that antibodies specific for GRP 78/BiP and PDI label the lumen of the RER and the surface of ICGs in situ and after their isolation, but do not label the interior of ICGs, is that GRP 78/BiP and PDI are excluded as the zymogens coaggregate. This conclusion is supported by the finding that GRP 78/BiP and PDI can be solubilized from isolated ICGs under nonreducing conditions in the absence (Fig. 8) and presence of SDS (Fig. 9), showing that they are restricted to the granules' surface and not disulphide bonded to the zymogens. If any GRP 78/BiP or PDI was present within the ICGs it should have been detected by immunocytochemistry. Although it is difficult to prove a negative, we are confident that the concentrations of GRP 78/BiP and PDI within the ICGs are below the threshold of detection by immunogold labeling and, therefore, below their concentrations in the lumen of the RER. It follows that the formation of ICGs at a neutral pH in the lumen of the RER is a sorting event which brings out of solution the set of zymogens in an aggregate while excluding PDI and GRP 78/BiP. PDI catalyzes disulphide exchange and, as a result, can restore the native conformation to a misfolded protein containing nonnative disulphide linkages (18). The mere fact that most of the zymogens in ICGs persist in a misfolded state provides further evidence that PDI does not reach the interior of the granules and act on the cross-linked zymogens.

Condensation before Cross-linking or Vice Versa

Does intermolecular cross-linking occur after the zymogens have condensed or is it concomitant with their condensation into ICGs? Of all the zymogens RNase alone apparently escapes extensive intermolecular cross-linking within the granules, and, as a result, more than half of the RNase in ICGs can be progressively eluted by four successive washes in buffered 2% SDS solution in the absence of a reducing agent. Therefore, at least one zymogen is incorporated into the ICGs without any intermolecular disulphide bonding. In addition we have shown that 10^{-2} and 10^{-3} M Co^{++} does not induce any immediate misfolding of newly synthesized zymogens in guinea pig pancreatic lobules. As far as can be judged from SDS-PAGE under nonreducing conditions zymogens synthesized in the presence and the absence of Co^{++} have the same conformation and in neither case are the proteins cross-linked by disulphide bonds. This indicates that Co^{++} does not inhibit PDI in vivo. We therefore favor the view that the intermolecular disulphide bonding is a consequence of coaggregation of the zymogens in the RER rather than its cause.

In vitro studies of disulphide bond formation indicate that

it is a relatively slow process in which partially native states containing incorrect disulphide bonds are formed on the pathway to the final equilibrium state, the native conformation (19). Often the rate of formation of the final state is much slower than the formation of one which has a great deal of native character but some nonnative disulphides (52). The role of PDI in the RER lumen is to catalyze the exchange of disulphides so that the equilibrium state is reached more rapidly. As a consequence, the rate of native disulphide bond formation is so rapid in vivo that a large fraction of the nascent chains acquire a partially native conformation. The native character of these still incompletely folded proteins is reflected in their ability to associate to oligomers within which intermolecular disulphide formation occurs. As in in vitro studies, larger proteins in vivo adopt their native conformations more slowly than smaller ones (40).

We propose that zymogens in partially native states are able to coaggregate to form ICGs from which PDI is excluded. The zymogens not yet in the equilibrium state and closely packed together in the ICGs can then exchange disulphides and form intermolecular covalent bonds cross-linking the content of the ICGs. The fact that RNase enters the aggregates in its native conformation and does not form intermolecular disulphide bonds is not surprising because it is the smallest zymogen and hence reaches its equilibrium state much more rapidly than the others (11, 13). In summary, we believe that the zymogens assume a sufficiently native state in the RER to allow them to coaggregate into ICGs. The cross-linking results from their sequestration from PDI before reaching their equilibrium state of disulphide bonding.

The alternative explanation that fully native proteins enter the ICGs and then form nonnative intermolecular disulphide bonds is unlikely. The native state of a protein is its lowest free energy state and, hence, the protein should not spontaneously rearrange to adopt a higher energy, nonnative state. Further, RNase which contains a free sulphhydryl in its native conformation should be incorporated into the disulphide-linked aggregate if the environment of the ICG promoted rearrangement of native disulphide bonds. Our data provide strong evidence that a large fraction of the zymogens occurs in the RER in their nonequilibrium states, because if the zymogens had reached their equilibrium before condensation into ICGs, cross-linking should not occur.

The remarkable exclusion of GRP 78/BiP from the interior of the ICGs can also be interpreted in favor of this conclusion. GRP 78/BiP binds to misfolded proteins in the RER (24, 26). If the initial condensation of zymogens into ICGs involved intermolecular disulphide bonding and, therefore, misfolding, one might expect GRP 78/BiP to remain bound to the zymogen molecules during the growth of the ICGs by surface accretion. GRP 78/BiP should therefore be present throughout the interior of the ICGs. That is not the case, which again suggests that the intermolecular disulphide bonding is not the cause of condensation but a secondary event.

Coordinate Induction of PDI, GRP 78/BiP, and GRP 94

The formation of ICGs represents the misfolding of proteins and their accumulation in the RER on a uniquely massive scale. The coordinate induction of GRP 78/BiP and GRP 94 after accumulation of malformed protein in the RER or treat-

ment of cells with calcium ionophore has been documented (26, 30). However, our results are the first to show that the synthesis of PDI is also induced along with that of the other two proteins. In this regard exocrine pancreatic cells clearly differ from plasmacytoma cells, in which induction of PDI was not observed when GRP 94 and GRP 78/BiP were induced (30).

Exclusion of PDI and GRP 78/BiP from Crystals

Whereas the formation of ICGs in guinea pig pancreas is a physiological event, the induction of amylase crystals in rat pancreas with injections of aromatic amino acids (5, 17) is not. The other methods of inducing these crystals in adult pancreas (49) or fetal rat pancreatic cells (41) are equally nonphysiological. Nevertheless the fact that these crystals include all of the zymogens, but exclude PDI and GRP 78/BiP which are present in amounts comparable to those of the least abundant zymogens, provides further evidence that the zymogens have the tendency to coaggregate to the exclusion of other proteins. Our data also indicate that amylase and the other zymogens in the crystals are in their native, equilibrium state. Hence, the molecular associations leading to the inclusion of all the zymogens in the crystals, and the exclusion of PDI and GRP 78/BiP are a property of the native conformation of this set of secretory proteins.

Condensation Sorting and Secretory Granule Formation

We chose to study condensation sorting in the RER of guinea pig and rat pancreatic cells, rather than in *trans* Golgi compartments of these or other cells, because we could obtain antibodies against abundant soluble resident proteins of the RER as well as against a set of regulated secretory proteins, the zymogens. Our results establish that condensation of secretory proteins into cores or crystals can sort them from abundant resident proteins in solution in the same compartment. This condensation sorting of pancreatic zymogens is not dependent upon an acidic environment or upon any other properties unique to the *trans* Golgi cisternae, including putative transmembrane receptor proteins. In the RER no further transport of the ICGs is achieved; they do not bud from the RER but move to autophagic vacuoles (25), presumably because this is the only route open to eliminate these insoluble disulphide-bonded aggregates.

We believe that the first step in the formation of authentic secretory granules is also condensation sorting of native proteins in condensing vacuoles. In the *trans* Golgi compartments condensation sorting is followed by the envelopment of the core of condensed secretory proteins with membranes that contains secretory granule-specific membrane proteins. This association of Golgi-derived membrane with granule cores may well involve specific transmembrane receptor proteins (8). However, we believe they are not required for the condensation of regulated secretory proteins into core structures.

We are grateful to Patricia Buck, Michael Hollingshead, and Ruth Jelinek for excellent technical assistance. We thank our colleagues Drs. Rainer Frank and Heinrich Gausepohl for synthesising the peptides used in this study. We thank Petra Riedinger and W. Mairs for help in preparing the figures and Helen Fry for typing the manuscript.

Received for publication 5 December 1988 and in revised form 1 March 1989.

References

- Anderson, R. G. W., and R. K. Pathak. 1985. Vesicles and cisternae in the *trans* Golgi apparatus of human fibroblasts are acidic compartments. *Cell*. 40:635-643.
- Anderson, R. G. W., J. R. Falck, J. L. Goldstein, and M. S. Brown. 1984. Visualization of acidic organelles in intact cells by electron microscopy. *Proc. Natl. Acad. Sci. USA*. 81:4838-4842.
- Balch, W. E., M. M. Elliott, and D. S. Keller. 1986. ATP-coupled transport of vesicular stomatitis virus of protein between the endoplasmic reticulum and the Golgi. *J. Biol. Chem.* 261:14681-14689.
- Bendayan, M., J. Roth, A. Perrelet, and L. Orci. 1980. Quantitative immunocytochemical localization of pancreatic secretory proteins in subcellular compartments of the rat acinar cell. *J. Histochem. Cytochem.* 28: 149-160.
- Bieger, W., and H. F. Hern. 1975. Studies on intracellular transport in the rat exocrine pancreas. I. Inhibition by aromatic amino acids *in vitro*. *Virchows Arch. A Pathol. Anat. Histol.* 367:289-305.
- Bradford, M. M. 1976. A rapid and sensitive method for the quantitation of microgram quantities of protein utilizing the principle of protein-dye binding. *Anal. Biochem.* 72:248-254.
- Broadwell, R. D., and C. Oliver. 1981. Golgi apparatus, GERL, and secretory granule formation within neurons of the hypothalamo-neurohypophysial system of control and hyperosmotically stressed mice. *J. Cell Biol.* 90:474-484.
- Burgess, T. L., and R. B. Kelly. 1987. Constitutive and regulated secretion of proteins. *Annu. Rev. Cell Biol.* 3:243-293.
- Burnette, W. N. 1981. "Western Blotting": electrophoretic transfer of proteins from sodium dodecyl sulfate-polyacrylamide gels to unmodified nitrocellulose and radiographic detection with antibody and radioiodinated protein A. *Anal. Biochem.* 112:195-203.
- Case, M. 1978. Synthesis, intracellular transport, and discharge of exportable proteins in the pancreatic acinar cell and other cells. *Biol. Rev. Camb. Philos. Soc.* 53:211-354.
- Creighton, T. E. 1978. Experimental studies of protein folding and unfolding. *Prog. Biophys. Mol. Biol.* 33:231-297.
- Desnuelle, P., and C. Figarella. 1979. Biochemistry. In *The Exocrine Pancreas*. H. T. Howat and H. Sarles, editors. W. B. Saunders Co., London. 86-125.
- Epstein, C. J., R. F. Goldberger, and C. B. Anfinsen. 1963. The genetic control of tertiary protein structure: studies with model systems. *Cold Spring Harbor Symp. Quant. Biol.* 28:439-449.
- Farquhar, M. G. 1969. Lysosome function in regulating secretion: disposal of secretory granules in cells of the anterior pituitary gland. In *Lysosomes in Biology and Pathology*. J. T. Dingle and H. B. Fell, editors. Elsevier North Holland Publishing Co. 462-482.
- Farquhar, M. G. 1971. Processing of secretory products by cells of the anterior pituitary gland. In *Sub-cellular Structure and Function in Endocrine Organs*. H. Heller and K. Lederis, editors. Cambridge University Press, Cambridge, England. 79-122.
- Farquhar, M. G., and G. E. Palade. 1981. The Golgi apparatus (complex) -(1954-1981)-from artifact to centerstage. *J. Cell Biol.* 91(No. 3, Pt. 2):77s-103s.
- Forssmann, W. G., and W. Bieger. 1973. Biosynthese falscher proteine: einbau von p-Cl-Phe in enzyme des exokrinen pankreas. *Res. Exp. Med.* 160:1-20.
- Freedman, R. B. 1984. Native disulphide bond formation in protein biosynthesis: evidence for the role of protein disulphide isomerase. *Trends Biochem. Sci.* 9:438-441.
- Freedman, R. B., and D. A. Hillson. 1980. Formation of disulphide bonds. In *The Enzymology of Post-Translational Modification*. R. B. Freedman and H. C. Hawkins, editors. Academic Press Inc., London. 158-212.
- Geuze, H. J., and J. W. Slot. 1980. Disproportional immunostaining patterns of two secretory proteins in guinea pig and rat exocrine pancreatic cells: an immuno-ferritin and fluorescence study. *Eur. J. Cell Biol.* 21:93-100.
- Griffiths, G., A. W. McDowall, R. Back, and J. Dubochet. 1984. On the preparation of cryosections for immunocytochemistry. *J. Ultrastruct. Res.* 89:65-78.
- Hopkins, C. R. 1972. The biosynthesis, intracellular transport, and packaging of melanocyte-stimulating peptides in the amphibian *pars intermedia*. *J. Cell Biol.* 53:642-653.
- Jamieson, J. D., and G. E. Palade. 1968. Intracellular transport of secretory proteins in the pancreatic exocrine cell. IV. Metabolic requirements. *J. Cell Biol.* 39:589-603.
- Kassenbroch, C. K., P. D. Garcia, P. Walter, and R. B. Kelly. 1988. Heavy-chain binding protein recognizes aberrant polypeptides translocated *in vitro*. *Nature (Lond.)*. 333:90-93.
- Kern, H. F., and D. Kern. 1969. Elektronenmikroskopische untersuchungen über die wirkung von kobaltchlorid auf das exokrine pankreas-

- gewebe des meerschweinchens. *Virchows Arch. ABT. B Zellpathol.* 4: 54-70.
26. Kozutsumi, Y., M. Segal, K. Normington, M. J. Gething, and J. Sambrook. 1988. The presence of malformed proteins in the endoplasmic reticulum signals the induction of glucose-regulated proteins. *Nature (Lond.)*. 332:462-464.
 27. Kreis, T. E. 1986. Microinjected antibodies against the cytoplasmic domain of vesicular stomatitis virus glycoprotein block in transport to the cell surface. *EMBO (Eur. Mol. Biol. Organ.) J.* 5:931-941.
 28. Lambert, N., and R. B. Freedman. 1983. Structural properties of homogeneous protein disulphide isomerase from bovine liver purified by a rapid high-yielding procedure. *Biochem. J.* 213:225-234.
 29. Louvard, D., H. Reggio, and G. Warren. 1982. Antibodies to the Golgi complex and rough endoplasmic reticulum. *J. Cell Biol.* 92:92-107.
 30. Macer, D. R. J., and G. L. E. Koch. 1988. Identification of a set of calcium binding proteins in reticuloplasm, the luminal content of the endoplasmic reticulum. *J. Cell Sci.* 91:61-70.
 31. Maizel, J. V., Jr. 1971. Polyacrylamide gel electrophoresis of viral proteins. *Methods Virol.* 5:179-224.
 32. McPherson, A., and A. Rich. 1972. X-ray crystallographic analysis of swine pancreas α -amylase. *Biochim. Biophys. Acta.* 285:493-497.
 33. Merisko, E. M., M. Fletcher, and G. E. Palade. 1986. The reorganization of the Golgi complex in anoxic pancreatic acinar cells. *Pancreas.* 1:95-109.
 34. Munro, S., and H. R. B. Pelham. 1986. An HSP-70-like protein in the ER: identity with the 78 kd glucose-regulated protein and immunoglobulin heavy chain binding protein. *Cell.* 46:291-300.
 35. Munro, S., and H. R. B. Pelham. 1987. A C-terminal signal prevents secretion of luminal ER proteins. *Cell.* 48:899-907.
 36. Orci, L., M. Ravazzola, and R. G. W. Anderson. 1987. The condensing vacuole of exocrine cells is more acidic than the mature secretory vesicle. *Nature (Lond.)*. 326:77-79.
 37. Palade, G. E. 1956. Intracisternal granules in the exocrine cells of the pancreas. *J. Biophys. Biochem. Cytol.* 2:417-422.
 38. Payan, F., R. Hasen, M. Pierot, M. Frey, and J. P. Astien. 1980. The three-dimensional structure of α -amylase from porcine pancreas at 5 Å resolution—the active site location. *Acta Cryst. Sect. B Struct. Sci.* 36:416-421.
 39. Pelham, H. R. B. 1988. Evidence that luminal ER proteins are sorted from secreted proteins in a post-ER compartment. *EMBO (Eur. Mol. Biol. Organ.) J.* 7:913-918.
 40. Peters, T., and L. K. Davidson. 1982. The biosynthesis of rat serum albumin, *in vivo* studies on the formation of the disulphide bond. *J. Biol. Chem.* 257:8847-8853.
 41. Rall, L., R. Pictet, S. Githens, and W. J. Rutter. 1977. Glucocorticoids modulate the *in vitro* development of the embryonic rat pancreas. *J. Cell Biol.* 75:398-409.
 42. Rausch, U., P. Vasiloudes, K. Rüdiger, and H. F. Kern. 1985. *In vivo* stimulation of rat pancreatic acinar cells by infusion of secretin. II. Changes in individual rates of enzyme and isoenzyme biosynthesis. *Cell Tissue Res.* 242:641-644.
 43. Reggio, H. A., and J. C. Dagorn. 1978. Ionic interactions between bovine chymotrypsinogen A and chondroitin sulfate A. B. C. *J. Cell Biol.* 78:951-957.
 44. Reggio, H. A., and G. E. Palade. 1978. Sulfated compounds in the zymogen granules of the guinea pig pancreas. *J. Cell Biol.* 77:288-314.
 45. Salpeter, M., and M. G. Farquhar. 1981. High resolution autoradiographic analysis of the secretory pathway in mammothrophs of the rat anterior pituitary. *J. Cell Biol.* 91:240-246.
 46. Scheele, G. A. 1975. Two-dimensional gel analysis of soluble proteins: characterization of guinea pig exocrine pancreatic proteins. *J. Biol. Chem.* 250:5375-5385.
 47. Scheele, G. A., and G. E. Palade. 1975. Studies on the guinea pig pancreas: parallel discharge of exocrine enzyme activities. *J. Biol. Chem.* 250: 2660-2670.
 48. Schick, J., H. F. Kern, and G. A. Scheele. 1984. Hormonal stimulation in the exocrine pancreas results in coordinate and anticordinate regulation of protein synthesis. *J. Cell Biol.* 99:1569-1574.
 49. Seybold, J., W. Bieger, and H. F. Kern. 1975. Studies on intracellular transport in the rat exocrine pancreas. II. Inhibition by anti-microtubular agents. *Virchows Arch. A Pathol. Anat. Histol.* 368:309-327.
 50. Tartakoff, A. M., and J. D. Jamieson. 1974. Subcellular fractionation of the pancreas. *Methods Enzymol.* 31:41-59.
 51. Tokuyasu, K. T. 1980. Immunocytochemistry in ultra-thin frozen sections. *Histochem. J.* 12:381-403.
 52. Wichman, A., A. Svenson, and L.-O. Anderson. 1977. The kinetics of refolding of completely reduced human serum albumin: regain of immunological reactivity. *Eur. J. Biochem.* 79:339-344.